Higher Surface Bowen Ratios Ineffective at increasing Updraft Intensity

Zachary R. Hansen[1] and Larissa E. Back[1]

Corresponding author: Zachary R. Hansen, Department of Atmospheric and Oceanic Sciences, University of Wisconsin-Madison, Madison, Wisconsin, USA. (zrhansen@wisc.edu)

[1]Department of Atmospheric and Oceanic Sciences, University of Wisconsin-Madison, Madison, Wisconsin, USA.

The sensitivity of various metrics of convective intensity to changes in boundary layer depth via changes in the surface Bowen ratio is explored with radiative-convective equilibrium (RCE) and initial condition simulations in the System for Atmospheric Modeling, a cloud resolving model (CRM). In the RCE simulations, high percentile updrafts showed little change in response to changes in the surface Bowen ratio. Initial condition simulations showed low surface Bowen ratios having stronger updrafts than high surface Bowen ratios. A parcel model was used to explore whether RCE results could be explained with an entrainment parameter independent of boundary layer depth. It was found that for every set of simulations in RCE, entrainment rates independent of boundary layer depth could explain the lack of change in updraft velocities with boundary layer depth. Given the indifference of high percentile updraft velocities in our simulations to changes in the surface Bowen ratio, we conclude that convective intensity as measured by this quantity in the cloud resolving model is not sensitive to this forcing.

1. Introduction

Tropical deep convection has large variations in the occurrence of high intensity convective storms over land versus over the ocean [*Zipser*, 2003]. This is seen in lightning flash rate measurements [*Cecil et al.*, 2014], as well as in the few direct measurements of updraft velocity from convective cumulus [*Lucas et al.*, 1994]. In general, lightning flash rate can be considered a good proxy for storm updraft velocity because it is thought that lightning flash rate increases monotonically with the updraft velocity of the storm [*Boccippio*, 2002]. Measurements of convective cumulus overshooting the tropopause have also been shown to be much more frequent over land than over ocean [*Liu and Zipser*, 2005]. Minimum brightness temperatures of the 37 and 85 GHz channels as observed from the Tropical Rainfall Measuring Mission Satellite, as well as the heights of 40 dBZ echo tops indicate that storms over land are stronger than those over the ocean [*Zipser et al.*, 2006]. In general, it seems that by many measures of intensity, from updraft velocity, to lightning flash rate, to overshooting top frequency, convective events over tropical landmasses tend to be much stronger than those over tropical oceans. It is our goal to test and explore one of the more popular hypotheses regarding what controls tropical convective intensity: the surface Bowen ratio (SBR) and by proxy, boundary layer depth using a cloud-resolving model. The $SBR = SHF/LHF$, where SHF is the sensible heat flux, and LHF is the latent heat flux.

Land surfaces typically experience a more notable diurnal cycle in temperature than oceans do, mainly due to the lower heat capacity of land. Therefore, it seems plausible that convective available potential energy (CAPE) over land could have larger values than over the oceans in the tropics. However, available data does not show a marked difference of CAPE between land and ocean: Observations are sparse, from one of the few publications available, CAPE does not vary too much between land and ocean [*Williams and Renno*, 1993]. Reanalysis data indicates some differences in mean CAPE between tropical continents and oceans, but they are within an order of magnitude, and over the maritime continent, CAPE has values very similar to nearby oceans, despite a very large difference in lightning activity in those regions [*Riemann-Campe et al.*, 2009; *Cecil et al.*, 2014]. *Lucas et al.* [1994] stated that there "is no basis at all for attributing updraft velocity differences [between various field campaigns] to CAPE over land and water." With that in mind, we explore a different hypothesis that could explain the observed land-ocean differences in lightning flash rate.

Variations of the fractional entrainment rate of environmental air into a rising moist parcel is a popular hypothesis for why intensity metrics like updraft velocity and lightning flash rate may be higher over landmasses than over oceans in the tropics [*Zipser*, 2003; *Williams and Stanfill*, 2002]. If there is less dilution of a parcel, it follows that intensity metrics related to moist buoyancy are larger than in cases when there is more dilution by drier environmental air [*Williams and Stanfill*, 2002]. Some researchers [*Lucas et al.*, 1994, 1996; *Zipser*, 2003; *Williams and Stanfill*, 2002; *Williams et al.*, 2005] have argued that entrainment rates over land and ocean could vary due to potential differences in updraft width. *Williams and Stanfill* [2002] described the concept that as boundary layer depth increases, the width of updrafts reaching cloud base increases, and with a wider updraft it is harder for environmental air to impinge into the updraft core, thus keeping the convective plume less diluted and more buoyant.

Boundary layer depth can be controlled by the surface Bowen ratio. If we consider the tropics to have a constant total surface flux, increasing the SBR will result in a deeper boundary layer. Typical values for ocean SBRs are around 0.05, while those over land tend to go from 0.25 and up [*Williams and Stanfill*, 2002]. Thus, boundary layer depth over land is greater than that over the ocean.

It has been found that one measure of convective intensity, lightning flash rate, is proportional to boundary layer depth [*Williams et al.*, 2005]. Ice water path, another variable that could influence lightning frequency has also been found to be strongly correlated with boundary layer depth [*Leung*, 2011]. *Williams and Stanfill* [2002] suggested that the influence of the SBR on boundary layer depths and hence updraft widths is a plausible control for land-ocean differences in convective intensity in the tropics. Comparison of updraft widths between GATE [*LeMone and Zipser*, 2005] and those of the Thunderstorm Project [*Byers and Braham*, 1949], showed that the updrafts over land were notably wider than those over the ocean. This combined support for the idea that regional variations in the surface Bowen ratio could lead to convective intensity differences via their influence on updraft width is what led us to test this hypothesis in a CRM framework.

Given the physical evidence indicating that deeper boundary layers resulting from higher SBRs might enhance convective intensity by limiting entrainment, this study focuses on examining this mechanism in a cloud-resolving model. Our simulations were used to test whether variations in SBR could control high percentile updraft velocities, a statistic that can be used as a corollary to convective intensity [as in e.g. *Lucas et al.*, 1994; *Zipser*, 2003].

Another intensity metric that we examine is frictional dissipation by falling precipitation and precipitation dissipation scale height [*Pauluis and Dias*, 2013], which is the former, normalized by precipitation, outputting a distance variable. Greater scale heights imply more recirculation of precipitation in convective cumulus, indicating that there may be more ice available to generate lightning. Previous work has shown that the precipitation scale height seems to effectively highlight a land-ocean convective intensity difference [*Pauluis and Dias*, 2013]. We also examine what we refer to as graupel dissipation and scale height, which is likely more directly applicable to the development of lightning.

We examine radiative-convective equilibrium [RCE, as in e.g. *Parodi and Emanuel*, 2009; *Singh and O'Gorman*, 2014], and initial condition simulations as in [*Robinson et al.*, 2011]. In examining all of our simulations, we asked the following questions:

- Does increasing the SBR in CRM simulations produce stronger high intensity updraft statistics?
- How do other convective intensity metrics vary?
- Does entrainment have to depend on the surface Bowen ratio to explain our results?

There are potential limitations to using RCE and cloud resolving models as a framework for measuring convective intensity. *Varble et al.* [2014] found that many cloud resolving models (including the model we use) attempting to replicate field campaign data overestimated vertical velocities in deep convective storms. Our goal isn't to reproduce real world convection, but to test the sensitivity of convection to major differences in surface forcing. While it's certainly possible that these models will not respond to forcings as deep convection responds in real life, they do include processes that should influence the response to variations in surface Bowen ratio. Hence it is of interest to see what they tell us about how surface Bowen ratios influence the intensity of deep convection, even if this will not definitively tell us about what real world convection would do. The methodology that we develop could be applied to other models when they are able to more accurately reproduce real-world convective intensities.

The methodology and setup for our cloud resolving model is described in section 2. Section 3 first presents intensity metrics directly from the CRM, and then uses a simple parcel model to explore the CRM environments. Section 4 discusses the potential implications of our results and concludes.

2. Methodology

Our simulations were conducted using the System For Atmospheric Modeling [SAM, version 6.10.3 *Khairoutdinov and Randall*, 2003]. Our tabulated simulations were run in both 2D and 3D, with horizontal resolutions of 200m in 3D, and 400m and 200m in 2D, always with 64 vertical levels. The model was run into radiative-convective equilibrium for the majority of cases, taking approximate 40 days. In all 2D simulations, the total run time was 50 days, while the 3D simulations had run times of 45 days in the low SBR case and 65 days in the high SBR case (as it took longer to reach RCE). The non-RCE cases were initial condition simulations, which were run for 1 model day, with statistics gathered over that day. All statistics were initially gathered at a 30 minute sampling interval.

All simulations used doubly or singly periodic boundary conditions with no Coriolis effect. All simulations utilized a 1.5 order subgrid-scale turbulence closure. In the simulations we show/tabulate results for, we used Morrison two-moment microphysics [*H. Morrison and Khvorostyanov*, 2005]. We also ran 2D and 3D simulations using Lin single-moment microphysics [*Yuh-Lang Lin and Orville*, 1983], including a 256km x 256km 1km resolution simulation where statistical convergence with domain size was reached (e.g. updraft statistics didn't change with doubled domain size). Because the qualitative results were generally the same, we show/tabulate a 3D, 200m Morrison microphysics runs with a domain size of 51.2km x 51.2km instead. In 2D, we were unable to achieve statistical convergence with domain size, and so ran domains of 410km and 820km for each set of resolutions. The qualitative results of the different domain sizes were the same, and so only the results from the 820km domain simulations in 2D will be shown here.

This study explores the impact of changing surface Bowen ratio, and by extension, boundary layer depth, on tropical convective intensity. For each combination of domain size and resolution, a control simulation meant to represent a tropical ocean is used with a fixed sea surface temperature (SST) of 300K. For each setup, we also run a simulation with a more land-like SBR and deeper boundary layer. Exact surface Bowen ratios and boundary layer depths of simulations are shown in table 1.

The SBR is altered by using an evaporative conductance parameter α inserted in the bulk equation for latent heat flux:

$$LHF = \alpha C_e |v| (q_s - q) \tag{1}$$

where LHF is the latent heat flux, C_e is the bulk transfer coefficient, $|v|$ is the magnitude of the wind speed at some height above the surface, q_s is the saturation specific humidity near the surface, and q is the near surface specific humidity. When α is 1, the SBR is at the standard oceanic value. As α decreases, latent heat flux is reduced.

Free tropospheric temperature is a known control on convective intensity [*Singh and O'Gorman*, 2014], and in the tropics horizontal temperature gradients in the free troposphere tend to be weak [*Charney*, 1963]. When the SBR and boundary layer depth of our simulations is increased by increasing α and maintaining the same SST, free tropospheric temperature falls. This is because a) the boundary layer follows the dry adiabat to higher heights in the high SBR case, and b) increased differences between SST and first model level temperature are needed in order for surface fluxes to balance radiative cooling. To account for this, we increase our SST in the high SBR cases in order to get all simulations' free tropospheric temperature to be nearly the same. Thus we fixed SSTs at 304K in for our high (land-like) SBR simulations. An iterative process was used to yield α values that gave free tropospheric temperatures that were nearly the same in each pair of varying α runs. For our high SBR simulations, we found an α value of 0.342 in the 2D cases, and an α value of 0.250 in the 3D case. The higher SBR runs had slightly higher free tropospheric temperatures (0.05K-0.50K) to exclude the possibility of low SBR cases having stronger high intensity updrafts due to a temperature difference.

Our setup for the initial condition simulations was much simpler: 3D, 200m resolution, 102.4 km x 102.4km domain size, interactive radiative cooling with Lin microphysics, and a TOGA COARE initial sounding, with no large scale tendencies. Instead of using an evaporative conductance parameter, we simply specified our sensible and latent heat fluxes for a total surface flux of 100 Wm^{-2} with SBRs of 0, 0.25, 0.5, and 1.

3. Results

3.1. Results from the CRM

The most intense updrafts of the high SBR cases were never stronger than those from the low SBR case. The top row of figure 1 shows a cumulative distribution function of 500 hPa instantaneous vertical velocity highlighting the upper tail of the distribution. At the 99.99th percentile, both cases have nearly the same vertical velocities, at odds with the initial hypothesis that thunderstorms with high SBRs have higher vertical velocities than those with low SBRs.

The bottom row of figure 1 shows maximum updraft velocity over a range of sampling intervals. There were no significant differences between simulation pairs, using a Mann-Whitney U test [*Mann and Whitney*, 1947] at the 95% significance level. The discrepancy in maximum vertical velocity between the 2D and 3D simulations may be explainable by the number of samples per time step being lower in the 2D simulations. Vertical profiles of buoyancy flux appear to be very similar over the entire troposphere, except in the boundary layer, which is to be expected given the different SBRs.

Inferred entrainment can be visualized from plots of the mass flux per moist static energy bin [*Pauluis and Mrowiec*, 2013], shown in figure 2. As we are interested in metrics of high intensity convection, we took the log of the mass flux, which highlights where rare parcel paths are occurring. Dilution of updrafts by environmental air can be described as follows:

$$\frac{dh_u}{dz} = \epsilon(h_{env} - h_u) \tag{2}$$

This gives the rate of change of the updraft moist static energy (MSE), h_u with height, z as a function of ϵ, entrainment rate, and environmental MSE, h_{env}. h_u is always larger than h_{env} for updrafts, meaning that entrainment decreases the buoyancy of convective plumes. Moist static energy is:

$$h = C_pT + gz + L_vq \tag{3}$$

Where h is the MSE, C_p is the specific heat capacity of dry air at constant pressure, T is the temperature, g is gravity, z is height above the surface, L_v is the latent heat of vaporization, and q is the specific humidity of water vapor.

By looking at the portions of the mass flux diagram with the highest moist static energies we can infer the which simulations are entraining more or less environmental air. If we assume entrainment rate is a known function of height, we can infer thermodynamic paths of the high MSE-air parcels. Because parcel MSE is controlled by the amount of entrainment experienced, higher MSE indicates lower entrainment rates and vice versa. For each pair of simulations, the maximum moist static energy of anomalously high MSE updrafts appears to be approximately the same, though the 3D & 2D 200m resolution simulations have slightly higher peak MSEs for the high SBR case, potentially indicating that some updrafts experiences slightly less entrainment than the low SBR case. These difference may also be due to the high SBR cases have slightly higher free tropospheric temperatures.

3.2. Precipitation Dissipation and related metrics

Precipitation dissipation in our simulations had no systematic response to changes in the SBR, as seen in table 1. However, when normalized by the surface precipitation, we see scale height differences that would suggest a land-ocean convective intensity difference, as one sees in lightning per unit precipitation observations. A caveat however: precipitation at cloud base is balanced by radiative cooling of the free troposphere [*O'Gorman et al.*, 2012], and the free troposphere shrinks when increasing the size of the boundary layer and maintaining free tropospheric temperature. Combined with the expectation of increased precipitation evaporation in a deeper boundary layer, it makes sense that when we normalize our precipitation dissipation by surface precipitation, we get larger values in the high SBR simulations.

Electric charges resulting in lightning are likely produced by collisions between graupel and small ice crystals in the presence of water droplets [pp 93, *Rakov and Uman*, 2003], so we examine a dissipation metric that only uses graupel, shown in Table 1. Frictional dissipation by graupel doesn't depend on SBR in a systematic way. We also calculated the graupel scale height by normalizing the graupel dissipation by the total falling precipitation at the lowest level of graupel existence. This graupel scale height shows a notable trend: high SBR cases have higher graupel scale heights than the low SBR cases. Thus there is more graupel dissipation per unit precipitation at freezing level, potentially providing a source for increased lightning that is independent of updraft velocity. Lin microphysics runs (not shown) did not show this tendency. It would be interesting to further explore the relationship of this metric to lightning in observations.

3.3. Initial Condition Simulations

In the initial condition simulations, we examined the mean maximum vertical velocity over the first day (30 minute sampling interval). For SBR 0, this metric was 39 ms^{-1}, for SBR 0.25: 37 ms^{-1}, for SBR 0.5: 34 ms^{-1}, and for SBR 1: 32 ms^{-1}. Hence, low SBR cases were notably stronger than high SBR cases. Other studies have suggested that idealized initial condition simulations can be used to produce results in line with real world observations of the intensity of convection as a function of island size [*Robinson et al.*, 2011], though the proposed mechanism is different than what we tested.

3.4. Analysis with Parcel Model

Our simulation pairs are producing high percentile updraft velocities that are very similar to one another. Using a 1-D parcel model, we check if the same distribution of entrainment rates gives similar vertical velocities in our simulation pairs to see if we can explain these results with an entrainment that is independent of boundary layer depth.

Undoubtedly, simple functions that approximate entrainment are not 100% correct. However they have received extensive use: in cumulus parameterizations [*Tokioka et al.*, 1988], for analysis from observations [*Holloway and Neelin*, 2009], as well as for the development of frameworks used to explain variations in convection [*Lucas et al.*, 1994; *Williams and Stanfill*, 2002; *Williams et al.*, 2005; *Singh and O'Gorman*, 2013].

We modified the 1-D parcel model from *Singh and O'Gorman* [2013] to use the environment from our RCE simulations to calculate entraining parcel paths. In the parcel model calculation, the parcel is lifted dry adiabatically to the lifting condensation level, then moist adiabatically to the level of neutral buoyancy. During moist ascent, entrainment occurs and modifies parcel moist static energy as in equation 2. Condensate loading is parameterized as a fraction of the total condensed water produced (30% for the figures). Total integrated buoyancy is calculated using the difference in density temperature between the environment and the parcel, and is integrated between the level of free convection (LFC) and the level of neutral buoyancy.

The following results use the 3D 200m resolution simulation pair. Other cases are qualitatively the same. Figure 3a shows the mean thermodynamic environment of our simulations along with two possible parcel paths with different fixed entrainment rates, ϵ (dashed lines). Figure 3b shows the difference in temperature between the high SBR simulation and the low SBR simulation, as well as their respective relative humidities as a function of height. Figure 3c shows potential maximum updraft velocity (square root of two times integrated buoyancy) as a function of fixed entrainment rate. Figure 3d shows maximum vertical velocity using an explicit vertical momentum equation [*Bretherton et al.*, 2004].

We first look at how well our parcel model produces the vertical velocity distributions seen in our CRM by using a range of specified ϵ. This is shown in figure 3c. Clearly, a fixed entrainment rate can give the same lack of variation in updraft velocity as was seen in figure 1.

The hypothesis that deeper boundary layers and higher SBRs have greater intensity due to larger updraft proportion [*Lucas et al.*, 1994, 1996; *Zipser*, 2003; *Williams and Stanfill*, 2002; *Williams et al.*, 2005] would be modeled with a function of entrainment that is inversely proportional to boundary layer depth:

$$\epsilon_{bl} = \frac{e}{Z_{bl}} \tag{4}$$

Where e is a specified entrainment parameter, and Z_{bl} is boundary layer depth. If this conceptual model were representative of what we see in our simulations, then we would expect differing ϵ_{bl} (by the factor $\frac{Z_{bl_{highSBR}}}{Z_{bl_{lowSBR}}}$), to produce the same vertical velocities in our simulation pairs. Clearly, that is not the case, as shown in figure 3c. Instead, the results of our simulations can be explained with a fixed entrainment rate that is independent of boundary layer depth.

Lower environmental relative humidities can lead to greater effective buoyancy in undilute plumes, potentially favoring a drier (more land-like) environment in the case of the most intense updrafts [*Singh and O'Gorman*, 2013]. The high and low SBR cases have very similar free tropospheric relative humidity. However, one might expect more land-like environments in nature to sometimes have lower free tropospheric humidities than occur over the ocean. It would be interesting to further explore the effects of environmental humidity on updraft velocities in the type of simulation setup we used here.

We looked at the sensitivity of the results shown in Figure 3c to condensate loading (from 0% - 100%), as well as our definition for the LFC, but found qualitatively the same general results, namely that for each pair of simulations, a fixed entrainment rate yields nearly the same vertical velocities. Variations on our LFC calculation that we used were a) defining the LFC as where the saturation moist static energy above the surface reached the value of the moist static energy of the surface, and b) looking for the level of maximum cloud water, as used in *Kuang and Bretherton* [2006].

Depending on the condensate loading used in the parcel model calculation, it appears possible that some updrafts may be undilute. Condensate loading values above approximately 70% give undilute maximum vertical velocity values around $55ms^{-1}$, which would coincide with an approximately 1 in 1,000,000 occurrence in our 3D simulations. These values are not observed in our 2D simulations, possibly because there are simply too few samples.

We also consider the effects of entrainment drag using the following explicit equation for vertical motion:

$$\frac{1}{2}\frac{\partial w^2}{\partial z} = aB - b\epsilon w^2 \tag{5}$$

where a and b are constants, and B is the buoyancy from the parcel model. Figure 3d shows maximum vertical velocities using parameters from *Bretherton et al.* [2004], setting $a = 1$ and $b = 2$. The magnitude of the maximum updraft velocity is much lower, but we are able to replicate maximum updraft velocities from figure 3c when altering the parameters. The distribution of updraft velocities as a function of entrainment rate tends to be similar between simulations using this model.

3.5. Cloud Widths

We checked the mean width of our clouds in these simulations by looking at the number of connected cloud water points at a given height, and calculating the area. For the 3D simulations we converted the area into an effective radius, while for 2D simulations, we used the width. As shown in table 1, the cloud widths at the lowest level of cloudiness were typically higher for the high SBR simulation, while cloud widths at the level of maximum cloudiness where generally very similar between simulation pairs. This might explain why our model wasn't producing differences in high intensity updraft statistics: differences in cloud width were the argument made by [*Williams and Stanfill*, 2002; *Williams et al.*, 2005] as to why storms over land entrain less than those over the ocean.

4. Discussion

Our goal was to test the hypothesis that land-like surface Bowen ratios contribute to observed convective intensity variations between land and ocean, including differences in lightning flash rate (updraft velocity by proxy). Our CRM simulations showed that changes in the SBR did not seem to produce notable differences in high percentile and maximum updraft velocities. Initial condition simulations produced weaker updrafts when SBRs were higher. Thus, in SAM, variations in the surface Bowen ratio do not produce the convective intensity differences that had previously been predicted, when intensity is described by updraft velocities.

The one metric that showed some response to variations in the SBR was the graupel scale height. These results imply that there may be some convective intensity metrics related to lightning flash rate that respond to SBR and are independent of vertical velocity. There were also some variations in the mass flux that indicated high SBR simulations may be entraining less, possibly allowing the high SBR case to have the same vertical velocities despite the higher undilute CAPE in the lower SBR simulations. However, variations in boundary layer depth are not strongly driving entrainment variations as these differences are small.

There are questions about the ability of CRMs to produce intense convection representative of real world processes [e.g. *Varble et al.*, 2014]. It is certainly possible that something nonphysical is preventing SAM from producing the expected updraft velocity difference in response to varying Bowen ratios. However, the model includes physics that leads to different boundary layer depths and cloud width differences at cloud base, so should be able to simulate the entrainment processes which have been hypothesized to lead to variations in updraft velocities. In the RCE simulations, cloud widths at the level of maximum cloudiness seem to be consistent with little dependence on SBR.

Analysis with a parcel model suggests that the updraft velocity results we are seeing are also consistent with entrainment not depending on SBR. A constant entrainment rate independent of boundary layer depth does a good job of approximating the lack of variation in vertical velocity seen in figure 1.

It remains to be seen what actually causes the convective intensity differences between land and ocean in the tropics. A more in-depth analysis of tropical CAPE distributions would be helpful in confirming that CAPE is not a controlling factor for regional variations in convective intensity. Diurnal cycles and the development and decay of convective inhibition could potentially predispose land surfaces towards more intense convection. Larger diurnal cycles occur over regions with higher SBRs, potentially explaining the observed relationship between boundary layer depth and convective intensity. Surface heterogeneities are another potential avenue of pursuit [*Rieck et al.*, 2014], which could potentially follow well with exploration of the surface Bowen ratio.

Acknowledgments. All data to reproduce figures is available from the authors upon request. Contact Zachary Hansen at zrhansen@wisc.edu. We would like to extend a big thanks to our anonymous reviewer whose in depth comments greatly strengthened the paper. This work was supported by NASA grant NNX12AL96G, L. Back startup funds from the University of Wisconsin, and the Advanced Opportunity Fellowship from the University of Wisconsin.

References

Boccippio, D. J. (2002), Lightning Scaling Relations Revisited, *Journal of the Atmospheric Sciences*, *59*(6), 1086–1104, doi:10.1175/1520-0469(2002)059¡1086:LSRR¿2.0.CO;2.

Bretherton, C. S., J. R. McCaa, and H. Grenier (2004), A New Parameterization for Shallow Cumulus Convection and Its Application to Marine Subtropical Cloud-Topped Boundary Layers. Part I: Description and 1D Results, *Monthly Weather Review*, *132*(4), 883–896, doi:10.1175/1520-0493(2004)132¡0883:ANPFSC¿2.0.CO;2.

Byers, H. R., and R. R. Braham (1949), The Thunderstorm Project, *U.S. Department of Commerce Tech. Rep.*, pp. 287–287.

Cecil, D. J., D. E. Buechler, and R. J. Blakeslee (2014), Gridded lightning climatology from trmm-lis and otd: Dadaset description, *Atmos. Res.*, *135*, 404–414, doi: 10.1016/j.atmosres.2012.06.028.

Charney, J. G. (1963), A Note on Large-Scale Motions in the Tropics, *Journal of the Atmospheric Sciences*, *20*(6), 607–609, doi:http://dx.doi.org/10.1175/1520-0469(1963)020¡0607:ANOLSM¿2.0.CO;2.

H. Morrison, J. A. C., and V. I. Khvorostyanov (2005), A New Double-Moment Microphysics Parameterization for Application in Cloud and Climate Models. Part I: Description, *J. Atmos. Sci.*, *62*, 16651677, doi:http://dx.doi.org/10.1175/JAS3446.1.

Holloway, C., and J. D. Neelin (2009), Moisture vertical structure, column water vapor, and tropical deep convection, *J. Atmos. Sci.*, pp. 1665–1683.

Khairoutdinov, M. F., and D. A. Randall (2003), Cloud resolving modeling of the arm summer 1997 iop: model formulation, results, uncertainties, and sensitivities, *J. Atmos. Sci.*, *60*, 607625, doi:http://dx.doi.org/10.1175/1520-0469(2003)060¡0607:CRMOTA¿2.0.CO;2.

Kuang, Z., and C. S. Bretherton (2006), A Mass-Flux Scheme View of a High-Resolution Simulation of a Transition from Shallow to Deep Cumulus Convection, *Journal of the Atmospheric Sciences*, *63*(7), 1895–1909, doi:10.1175/JAS3723.1.

LeMone, M. A., and E. J. Zipser (2005), Cumulonimbus vertical velocity events in GATE. Part I: Diameter, intensity and mass flux, *J. Atmos. Sci.*, *37*, 2444–2457, doi:10.1016/j.atmosres.2004.11.009.

Leung, W. Y. (2011), Potential Reduction of Uncertainty in Passive Microwave Precipitation Retrieval by the Inclusion of Dynamical and Thermodynamical Constraints as the Cloud Dynamics Radiation Database Approach.

Liu, C., and E. J. Zipser (2005), Global distribution of convection penetrating the tropical tropopause, *Journal of Geophysical Research: Atmospheres*, *110*(23), 1–12, doi:10.1029/2005JD006063.

Lucas, C., E. J. Zipser, and M. A. LeMone (1994), Vertical veloctiy in oceanic convection off tropical australia, *J. Atmos. Sci.*, *51*, 3183–3193, doi:10.1175/1520-0469(1994)051¡3183:VVIOCO¿2.0.CO;2.

Lucas, C., E. J. Zipser, and M. a. Lemone (1996), Reply, pp. 1212–1214, doi: http://dx.doi.org/10.1175/1520-0469(1996)053¡1212:R¿2.0.CO;2.

O'Gorman, P. a., R. P. Allan, M. P. Byrne, and M. Previdi (2012), Energetic Constraints on Precipitation Under Climate Change, *Surveys in Geophysics*, *33*(3-4), 585–608, doi: 10.1007/s10712-011-9159-6.

Parodi, A., and K. Emanuel (2009), A Theory for Buoyancy and Velocity Scales in Deep Moist Convection, *Journal of the Atmospheric Sciences*, *66*(1993), 3449–3463, doi:10.1175/2009JAS3103.1.

Pauluis, O. M., and J. Dias (2013), Satellite Estimate of Precipitation-Induced Dissipation in the Atmosphere, *Science*, *335*(February 2012), 953–957.

Pauluis, O. M., and A. Mrowiec (2013), Isentropic Analysis of Convective Motions, *Journal of the Atmospheric Sciences*, *70*(11), 3673-3688.

Rakov, V., and M. Uman (2003), *Lightning: Physics and Effects*, Cambridge University Press.

Riemann-Campe, K., K. Fraedrich, and F. Lunkeit (2009), Global climatology of Convective Available Potential Energy (CAPE) and Convective Inhibition (CIN) in ERA-40 reanalysis, *Atmospheric Research*, *93*(1-3), 534–545, doi:10.1016/j.atmosres.2008.09.037.

Robinson, F. J., S. C. Sherwood, D. Gerstle, C. Liu, and D. J. Kirshbaum (2011), Exploring the landocean contrast in convective vigor using islands, pp. 602–618, doi: 10.1175/2010JAS3558.1.

Siebesma, a. P., P. M. M. Soares, and J. a. Teixeira (2007), A Combined Eddy-Diffusivity Mass-Flux Approach for the Convective Boundary Layer, *Journal of the Atmospheric*

Sciences, *64* (4), 1230–1248, doi:10.1175/JAS3888.1.

Singh, M. S., and P. a. O'Gorman (2013), Influence of entrainment on the thermal stratification in simulations of radiative-convective equilibrium, *Geophysical Research Letters*, *40* (16), 4398–4403, doi:10.1002/grl.50796.

Singh, M. S., and P. a. O'Gorman (2014), Increases in moist-convective updraught velocities with warming in radiative-convective equilibrium, pp. n/a–n/a, doi:10.1002/qj.2567.

Tokioka, T., K. Yamazaki, a. Kitoh, and T. Ose (1988), The Equatorial 30-60 day Oscillation and the Arakawa-Schubert Parameterization, *Journal of the Meteorological Society of Japan*, *66* (6), 883–901.

Varble, A., E. J. Zipser, A. M. Fridlind, P. Zhu, A. S. Ackerman, J.-p. Chaboureau, S. Collis, J. Fan, A. Hill, and B. Shipway (2014), Evaluation of cloud-resolving and limited area model intercomparison simulations using TWP-ICE observations: 1. Deep convective updraft properties, *J. Geophys. Res. Atmos*, *119* (24), 13,891–13,918, doi:10.1002/2013JD021371.Received.

Williams, E., and N. Renno (1993), An analysis of the conditional instability of the tropical atmosphere, *Mon. Wea. Rev.*, *121*, 2136, doi:http://dx.doi.org/10.1175/1520-0493(1993)121¡0021:AAOTCI¿2.0.CO;2.

Williams, E., and S. Stanfill (2002), The physical origin of the landocean contrast in lightning activity, *Comptes Rendus Physique*, *3* (10), 1277–1292, doi:http://dx.doi.org/10.1016/S1631-0705(02)01407-X.

Williams, E., V. Mushtak, D. Rosenfeld, S. Goodman, and D. Boccippio (2005), Thermodynamic conditions favorable to superlative thunderstorm updraft, mixed phase microphysics and lightning flash rate, *Atmospheric Research*, *76*, 288–306, doi: 10.1016/j.atmosres.2004.11.009.

Yuh-Lang Lin, R. D. F., and H. D. Orville (1983), Bulk Parameterization of the Snow Field in a Cloud Model, *J. Climate Appl. Meteor.*, *22*, 10651092, doi: http://dx.doi.org/10.1175/1520-0450(1983)022¡1065:BPOTSF¿2.0.CO;2.

Zipser, E. J. (2003), Some views on hot towers after 50 years of tropical field programs and two years of trmm data, *Meteor. Monogr.*, *29*, 4949, doi: http://dx.doi.org/10.1175/0065-9401(2003)029¡0049:CSVOHT¿2.0.CO;2.

Zipser, E. J., D. J. Cecil, C. Liu, S. W. Nesbitt, and D. P. Yorty (2006), Where are the most intense thunderstorms on Earth?, *Bulletin of the American Meteorological Society*, *87*(8), 1057–1071, doi:10.1175/BAMS-87-8-1057.

Mann, H. B., and D. R. Whitney (1947), On a Test of Whether one of Two Random Variables is Stochastically Larger than the Other, *Ann. Math. Statist.*, *18*(1), 50–60, doi:10.1214/aoms/1177730491. http://projecteuclid.org/euclid.aoms/1177730491.

Rieck, M., C. Hohenegger, and C. C. van Heerwaarden (2014), The Influence of Land Surface Heterogeneities on Cloud Size Development, *Monthly Weather Review*, *142*, 3830–3846, doi:doi:10.1175/MWR-D-13-00354.1

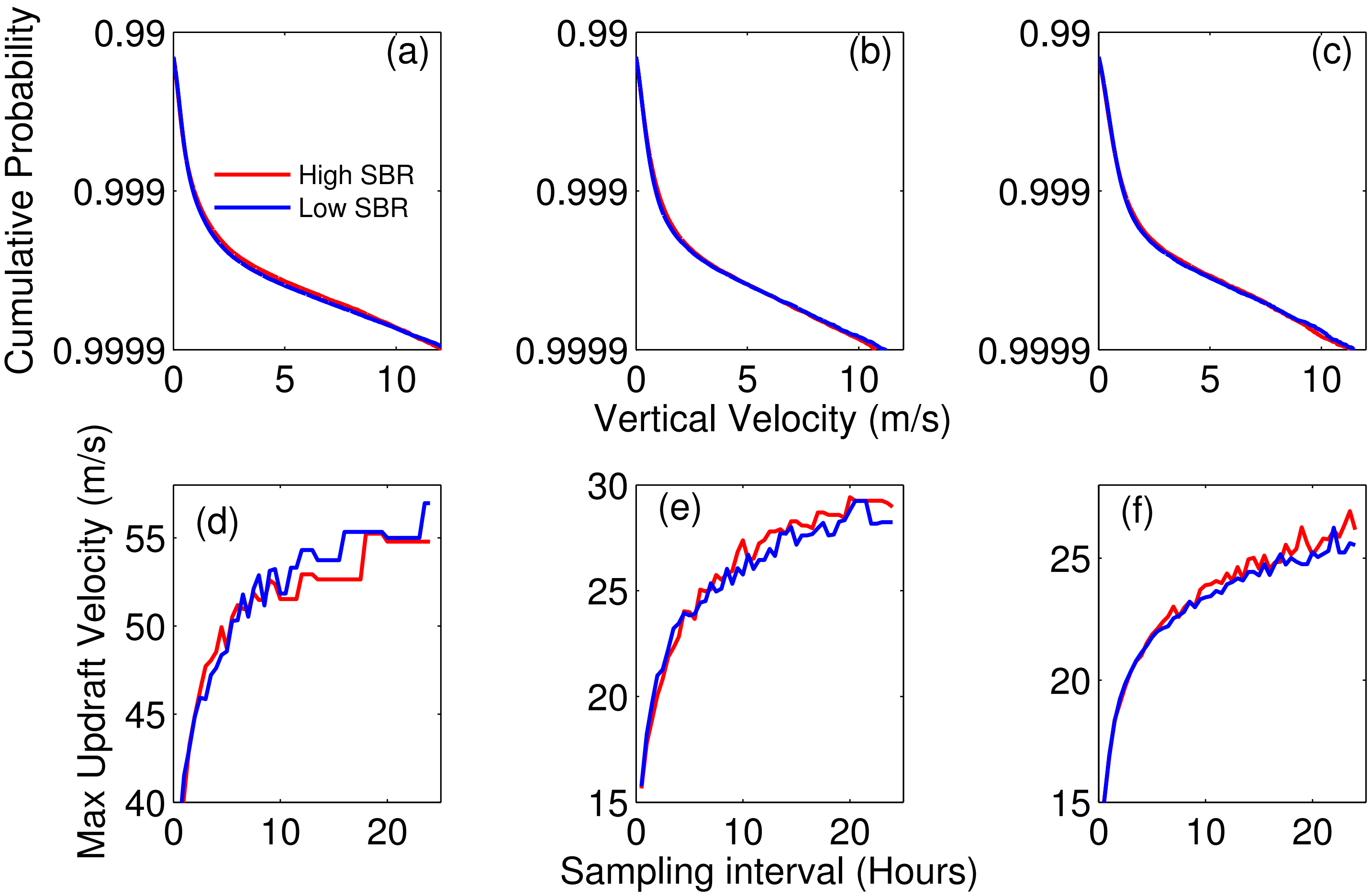

Figure 1. Cumulative distribution function of 500hPa vertical velocity (top row) and maximum updraft velocity as a function of sampling interval (bottom row). Red lines represent high or land-like SBR cases, while blue lines represent low or ocean-like SBR cases. (a) and (d) are 3D 200m resolution Morrison microphysics case, (b) and (e) are the 2D 400m resolution Morrison microphysics case, (c) and (f) are the 2D 200m resolution Morrison microphysics case.

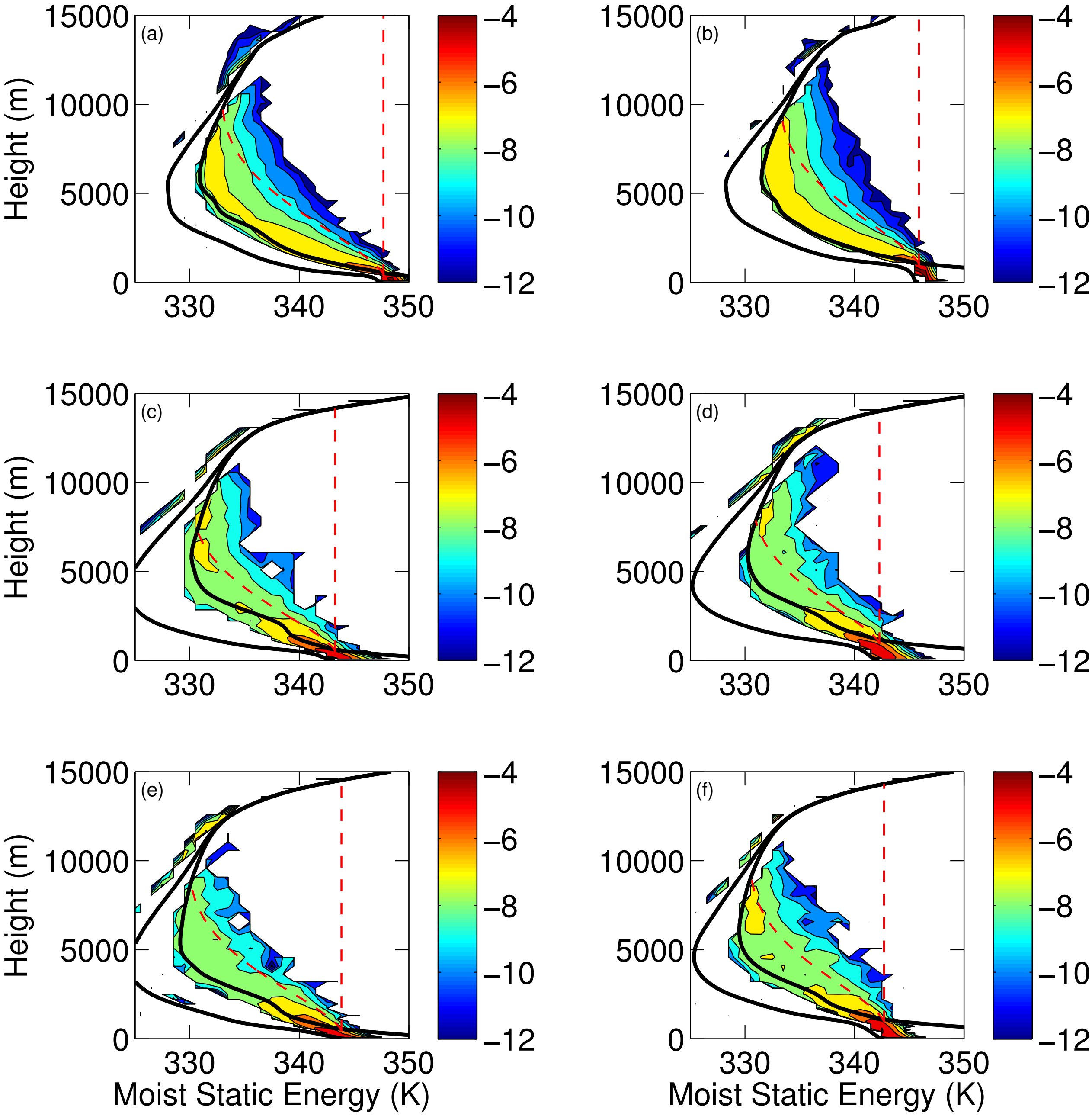

Figure 2. Log of positive mass flux per 1K MSE bin vs height for low SBR cases (left column) and high SBR cases (right column). Black lines are MSE and saturation MSE, while red dashed lines show potential entraining parcel paths with fixed entrainment rates of 0 and 0.3 km^{-1}. (a) and (b) are 3D 200m resolution Morrison microphysics, (c) and (d) are 2D 400m resolution Morrison microphysics simulations, (e) and (f) are 2D 200m resolution Morrison microphysics simulations.

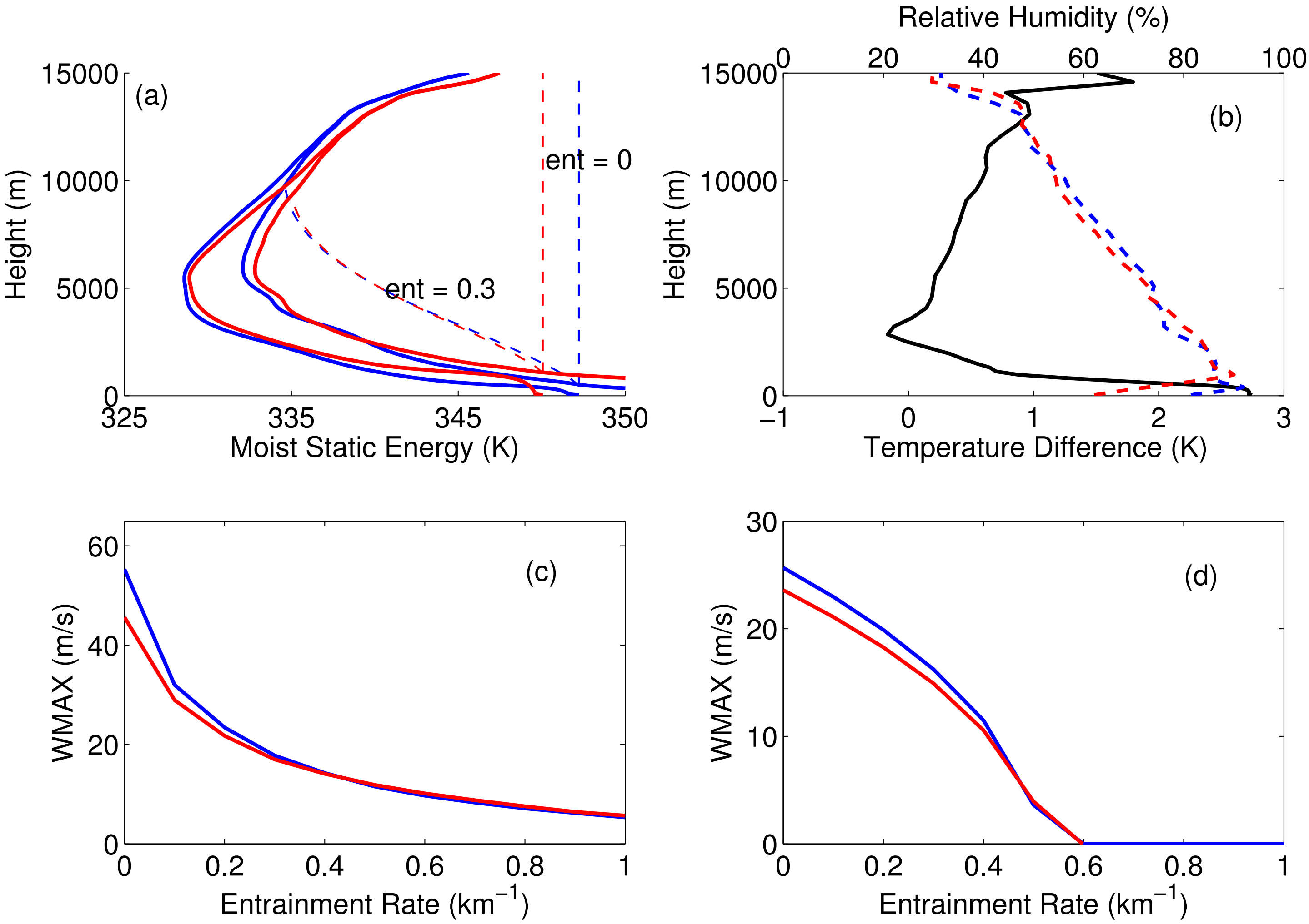

Figure 3. Thermodynamic characteristics, and results from the entraining parcel model for the 3D 200m resolution simulations. (a) Shows the thermodynamic diagram as in figure 2, but for both high and low SBR, where *ent* is a fixed entrainment rate (km^{-1}). (b) The temperature difference between the high SBR case and the low SBR case (black line) and their respective relative humidities (dashed lines). (c) and (d) give potential maximum updraft velocity as a function of entrainment rate. (c) integrates buoyancy to produce maximum vertical velocity, and (d) shows maximum calculated vertical velocity from the explicit vertical velocity equation. Red lines represent the high or land-like SBR case, while blue lines represent low or ocean-like SBR case.

Simulation	SBR	BLD	D_P	D_G	SH_P	SH_G	X_{Cl}	X_{Cmax}
3D 200m Morrison Low SBR	0.08	475	1.09	0.51	3.93	8.76	1.30	1.70
3D 200m Morrison High SBR	0.39	1025	1.22	0.60	5.45	13.3	1.49	1.64
2D 400m Morrison Low SBR	0.08	575	2.37	0.39	6.33	5.87	0.80	1.4
2D 400m Morrison High SBR	0.23	1025	2.00	0.53	7.83	8.32	1.1	1.4
2D 200m Morrison Low SBR	0.08	525	1.09	0.39	3.70	5.17	1.0	1.7
2D 200m Morrison High SBR	0.23	975	1.00	0.37	4.60	6.43	1.3	1.6

Table 1. The surface Bowen ratio (SBR), boundary layer depth (BLD (m)) defined by the height of the lifting condensation level, precipitation and graupel dissipation (D_P and D_G respectively) as well as their scale heights (SH_P and SH_G), and cloud widths (2D simulation) or effective radius (3D simulation) at the lowest level of cloudiness (X_{Cl}) and the level of maximum cloudiness (X_{Cmax}) for each of the three simulation pairs. Boundary layer depth is meters, dissipation is in units of watts per meter squared and scale height is in units of kilometers. Cloud width is in units of kilometers.